Computational and Applied Mathematics (2019) 38:162
https://doi.org/10.1007/s40314-019-0952-z

Gegenbauer wavelet operational matrix method for solving variable-order non-linear reaction–diffusion and Galilei invariant advection–diffusion equations

Sachin Kumar[1] · **Prashant Pandey**[1] · **Subir Das**[1]

Received: 1 April 2019 / Revised: 1 July 2019 / Accepted: 24 September 2019 /
Published online: 4 October 2019

Abstract
In this article, a variable-order operational matrix of Gegenbauer wavelet method based on Gegenbauer wavelet is applied to solve a space–time fractional variable-order non-linear reaction–diffusion equation and non-linear Galilei invariant advection diffusion equation for different particular cases. Operational matrices for integer-order differentiation and variable-order differentiation have been derived. Applying collocation method and using the said matrices, fractional-order non-linear partial differential equation is reduced to a system of non-linear algebraic equations, which have been solved using Newton iteration method. The salient feature of the article is the stability analysis of the proposed method. The efficiency, accuracy and reliability of the proposed method have been validated through a comparison between the numerical results of six illustrative examples with their existing analytical results obtained from literature. The beauty of the article is the physical interpretation of the numerical solution of the concerned variable-order reaction–diffusion equation for different particular cases to show the effect of reaction term on the pollution concentration profile.

Keywords Fractional PDE · Variable-order diffusion equation · Operational matrix · Gegenbauer wavelet · Collocation method

Mathematics Subject Classification 35R11 · 34A08 · 41A10

Communicated by José Tenreiro Machado.

✉ Sachin Kumar
sachinraghav522@gmail.com

Prashant Pandey
ppunique1133@gmail.com

Subir Das
sdasapm@iitbhu.ac.in

[1] Department of Mathematical Sciences, Indian Institute of Technology (B.H.U), Varanasi 221005, India

1 Introduction

Fractional calculus is an ancient topic of mathematics with history as ordinary or integer calculus (Machado et al. 2011). It is developing progressively now. The theory of fractional calculus was developed by Abel and Liouville. The details can be found in Kilbas et al. (2006), Podlubny (1998). In the last few years, fractional calculus has attracted the attention of the researchers of medical physics, chemistry, biology, engineering and mathematics. Fractional calculus and fractional differential equation are found in many applications in different fields (Milici et al. 2019). Many different forms of fractional-order differential operators were introduced as the Grunwald–Letnikov, Riemann–Liouville, Hadamard, Caputo, Riesz and variable-order fractional operators. Due to its increasing applications, researchers have paid their attention to find numerical and exact solutions of the fractional-order differential equations. As there are many difficulties in solving a fractional-order differential equation by analytic method, there is a need of seeking numerical solutions. There are many numerical methods available in literature, viz., eigenvector expansion, Adomain decomposition method (Suarez and Shokooh 1997), fractional differential transform method (Darania and Ebadian 2007), homotopy perturbation method (Hashim et al. 2009), predictor–corrector method (Diethelm et al. 2002) and generalized block pulse operational matrix method (Li and Sun 2011), etc. Some numerical methods based upon operational matrices of fractional-order differentiation and integration with Legendre wavelets (Jafari et al. 2011), Chebyshev wavelets (Yuanlu 2010), sine wavelets, and Haar wavelets (Li and Zhao 2010) have been developed to find the solutions of fractional-order differential and integro-differential equations. The functions which are commonly used include Legendre polynomial (Odibat 2011), Laguerre polynomial (Gürbüz and Sezer 2016), Chebyshev polynomial and semi-orthogonal polynomial such as Genocchi polynomial.

Samko and Ross (1993) have investigated fractional operator when the order is variable during many physical processes. This generalization of fractional derivative to be a non-constant depending on time and space is very interesting. This approach of variable-order fractional calculus has numerous applications in physics, mechanics, control and signal processing (Soon et al. 2005; Valério and Sá da 2013; Ortigueira et al. 2019). There are many definitions of variable-order fractional derivative and integration. The variable-order operators have too complex kernel for having a variable exponent. So, to find numerical solution of variable-order fractional differential equation (VOFDE) is a little bit tough task as compared to constant-order differential equation. In article Coimbra (2003), a consistent approximation is used to solve VOFDE. A finite difference scheme to find the solution of VOFDE and convergence analysis is used in article (Lin et al. 2009). Some latest and updated methods are discovered to find the numerical solution of VOFDE, viz., finite difference method (Moghaddam and Machado 2017b; Moghaddam and Mostaghim 2017), B-linear spline method (Machado and Moghaddam 2018), cubic spline method (Moghaddam and Machado 2017a, c), integro quadratic spline interpolations (Moghaddam et al. 2017; Keshi et al. 2018) and spectral method (Moghaddam et al. 2019). Analytic solution of variable-order differential equation is given in article Malesza et al. (2019). Variable-order fractional Laplacian equation with variable growth has been solved in article Xiang et al. (2019). In article Zayernouri and Karniadakis (2015), spectral collocation method is proposed to solve some linear and non-linear VOFPDE. An accurate discretization technique has been developed in Hajipour et al. (2019) to solve variable-order fractional reaction–diffusion problems.

Reaction–diffusion process has been investigated for a long time. In the process of reaction–diffusion, reacting molecules are used to move through space due to diffusion.

This definition excludes other modes of transports such as convection and drift that may arise due to the presence of externally imposed fields.

When a reaction occurs within an element of space, molecules can be created or consumed. These events are added to the diffusion equation and lead to reaction–diffusion equation of the form

$$\frac{\partial c}{\partial t} = D\nabla^2 c + R(c,t), \tag{1}$$

where $R(c,t)$ denotes the reaction term at time t. The extension of the reaction–diffusion equation in fractional-order system can be found in the articles (Das et al. 2011; Jaiswal et al. 2018; Das et al. 2018; Tripathi et al. 2016). In nature, many of the beautiful systems in biology, physics,chemistry, and physiology can be described by reaction–diffusion equations. For example, the distribution and organization of vegetation-like bushes in arid ecosystems (Couteron and Lejeune 2001), the stripes and spots on fish (Kondo and Asai 1995), snakes (Murray 1981) and the skin or fur of mammals (Kondo 2009) have been studied by the standing waves which are produced by reaction–diffusion equations.

The advection–diffusion equation is a combination of diffusion and convection. The transport of material by a known velocity field can be described by the reaction–advection diffusion equation (RADE). The general form of this equation is

$$\frac{\partial u(x,t)}{\partial t} = \nabla.(C\nabla u) - \nabla.(\nu u) + R,$$

where $u(x,t)$ is a variable representing the concentration of mass transfer and temperature of heat transfer. C is the diffusion coefficient and ν is the velocity of the fluid flow as a function of time and location.

The fractional-order reaction advection–diffusion equation (RADE) is a generalized version of classical RADE. Many physical phenomena such as transport dynamics in complex system, glassy and porous media, geological and geophysical processes can be modeled by the advection–diffusion equation. Einstein's theory of Brownian motions reveals that the mean square displacement of a particle moving randomly is proportional to time. Thus in the fundamental solution of the integer-order transport equation, the probability density function governing the Brownian motion will be Gaussian type whose mean square displacement is $\langle X^2(t)\rangle \sim t$, and if the integer-order transport equation is extended to the time-fractional-order system, then the phenomena of anomalous diffusion are observed. Therefore after the advancement of fractional calculus, it is seen that the mean square displacement for an anomalous diffusion equation having time-fractional derivative grows slowly with time. For the simple fractional-order diffusion equation $\frac{\partial^\alpha u}{\partial t^\alpha} = \frac{\partial^2 u}{\partial x^2}$, the mean square displacement is $X^2(t) \sim t^\alpha$, where α is the anomalous diffusion exponent. An important characteristic of this evolution equation is that it generates the fractional Brownian motion, a generalization Brownian motion. Thus if we replace the integer-order derivative with the fractional one, it changes the fundamental concept of time and the concept of evolution in the foundations of physics. The fractional-order derivative has a physical meaning related to the statistics of waiting times according to the Montroll–Weiss theory. It can also be shown that for fractional-order reaction advection–diffusion equation (RADE), the mean square displacement will be $\langle X^2(t)\rangle \sim t^{\frac{3\alpha}{2}}$, $0 < \alpha < 1$ and thus we can say that the transportation equation of the form of RADE follows the evolutionary process.

In the last two decades, fractional differential equation have been widely used by researchers not only in science, engineering, economics and finance, but also helps in modeling multiscale problems, characterized by wide or length scale. The excellence of the

fractional-order differential operator is its nonlocal property, which takes into account the fact that the future state not only depends upon the present state, but also upon all the history of its previous states. Nowadays, the fractional-order system has gained popularity in the investigation of dynamical system, since it allows greater flexibility in the model. The main advantage of the fractional calculus is that it provides an excellent instrument for the description of the memory effect of various physical processes. The derivatives and integrals of fractional order are useful to explore the characteristic features of anomalous diffusion, transport and fractal walks through setting up of fractional kinetic equations, which are useful in anomalous sub-diffusion. Stability analysis of the variable-order FDE is complex, but the authors have made an endeavor to show the stability of ultraspherical wavelets expansion used to solve the concerned problem. Recent studies of fixed-order FDEs show that they are unable to characterize the adequate information on complex natural phenomena, viz, complex diffusion occurring in heterogeneous disordered porous media. So there are a lot of limitations of applying fractional differential order during modeling. To overcome the limitations, the concept of variable-order operators has been introduced. Thus, generalization of fixed order to VO operator provides a new perspective to describe the said mathematical complex systems (Dabiri et al. 2018).

The Gegenbauer polynomial and wavelet (Rehman and Saeed 2015; Elgindy and Smith-Miles 2013) are generalization of Legendre and Chebyshev polynomials and wavelet, which have been used in the present article to solve non-linear variable-order reaction–diffusion equation and non-linear variable-order Galilei invariant advection–diffusion equation. After finding the operational matrix of fractional differentiation of integer and variable order, we collocate the given non-linear fractional-order model and boundary conditions. By collocating we get a non-linear system of algebraic equations which are solved by using an iteration method called Newton method. To validate the accuracy and efficiency of the proposed method, the numerical results obtained by solving different particular forms of two given models under the prescribed initial and boundary conditions are compared with the exact solutions and the results are presented through graphs and tables. The article is organized as follows.

In Sect. 2, the definitions, mathematical preliminaries of fractional calculus, Gegenbauer polynomial, Gegenbauer wavelet and their properties are given. Section 3 continues with function approximation. In Sect. 4, the error bound and convergence analysis for the proposed method have been investigated. In Sect. 5, the operational matrices of differentiation for integer and variable orders by Gegenbauer wavelet have been derived. The validation of the method through a comparison of the numerical results with the existing analytical results for the six particular cases of two given models is given in Sect. 8. The conclusion of over all work is presented in Sect. 9.

2 Preliminaries

Here, few definitions and important properties of fractional calculus have been introduced. In literature, definitions of two types of variable-order derivative have been introduced. These two definitions are named as variable-order derivative type 1 (V1) and variable-order derivative type 2 (V2). Here, the definition suggested in Coimbra (2003), Moghaddam and Machado (2017a) has been used.

2.1 Definitions of variable-order derivatives of type 1 (V1) and type 2 (V2)

Type 1 (V1) variable-order fractional derivative of order $q-1<\vartheta(t)\leq q$ of a function $u(x,t)$ with respect to variable t is defined as (Lv and Xu 2016)

$$ {}_0D_t^{\vartheta(t)}u(x,t)=\begin{cases}\dfrac{1}{\Gamma(q-\vartheta(x,t))}\int_0^t(t-s)^{q-\vartheta(x,t)-1}\dfrac{\partial^q u(x,t)}{\partial s^q}\mathrm{d}s, & q-1<\vartheta(t)<q,\\ \dfrac{\partial^q u(x,s)}{\partial s^q}, & \vartheta(t)=q.\end{cases} \tag{2}$$

Here if $\vartheta(t)$ is constant, then this definition is equivalent to constant-order fractional derivative in Caputo sense (Tavares et al. 2016). From this definition, it can be shown that memory effect of a given system is changed with time and can be determined by its current state. So, variable-order definition is useful to characterize variable memory effect of the system. Type 1 (V1) form of variable-order operator is useful to depict properly different real-world diffusion processes. From the definition, it can be easily seen that the variable-order fractional derivative follows the linear property

$$ {}_0D_t^{\vartheta(t)}(c_1f(x,t)+c_2g(x,t))=c_1\ {}_0D_t^{\vartheta(t)}f(x,t)+c_2\ {}_0D_t^{\vartheta(t)}g(x,t). \tag{3}$$

It has the following useful property:

$$ {}_0D_t^{\vartheta(t)}t^m=\begin{cases}\dfrac{\Gamma(m+1)}{\Gamma(m-\vartheta(t)+1)}t^{m-\vartheta(t)}, & q\leq m,\\ 0, & \text{otherwise.}\end{cases} \tag{4}$$

The type V2 of variable-order differential operator is defined as

$$ {}_0D_t^{\vartheta(t)}u(x,t)=\begin{cases}\int_0^t\frac{(t-s)^{q-\vartheta(x,s)-1}}{\Gamma(q-\vartheta(x,s))}\frac{\partial^q u(x,t)}{\partial s^q}\mathrm{d}s, & q-1<\vartheta(t)<q,\\ \frac{\partial^q u(x,s)}{\partial s^q}, & \vartheta(t)=q.\end{cases} \tag{5}$$

In article Sun et al. (2011), it is shown that fractional derivative shows the long memory effect of a system and memory effect is reduced as the order approaches the integer order. The consequences represent that memory effect depicted by V1 type operator model changes with fast rate as compared to the model containing V2 type operator model. Since a model of V2 type contains the memory of its history, it prevents the system behavior from changing sharply. When defining the variable-order operational matrix, we use the relation (4). If we choose the V2 type operator, then due to the integrand $\frac{(t-s)^{q-\vartheta(x,s)-1}}{\Gamma(q-\vartheta(x,s))}\frac{\partial^q u(x,t)}{\partial s^q}$, the integration in the definition becomes too complicated to solve analytically. Thus, the operational matrix of operator V1 is easy to compute as compared to V2 type and saves a lot of computational time. On the other hand, if we use type 2 derivative, then we have to adopt a suitable numerical integration scheme to compute the complicated integration, which may give us less accurate results as compared to the results obtained by using V1 type derivative.

2.2 Gegenbauer polynomial and Gegenbauer wavelet

The Gegenbauer polynomials also known as ultraspherical harmonics polynomials denoted by $G_\lambda^n(x)$, for $\lambda>\frac{-1}{2}$, satisfy the following singular Sturm–Liouville equation on $[-1,1]$ as

$$ \frac{\mathrm{d}}{\mathrm{d}y}\left[(1-y^2)^{\lambda+\frac{1}{2}}\frac{\mathrm{d}}{\mathrm{d}y}G_\lambda^n(y)\right]+n(n+2\lambda)(1-y^2)^{\lambda-\frac{1}{2}}G_\lambda^n(y)=0. \tag{6}$$

These polynomials can also be derived by the following recurrence relations

$$G_\lambda^0(y) = 0, G_\lambda^1(y) = 2\lambda y,$$
$$G_\lambda^{n+1}(y) = \frac{1}{n+1}[2y(\lambda+n)G_\lambda^n(y) - (2\lambda+n-1)G_\lambda^{n-1}(y)].$$

The Rodrigues formula to compute the Gegenbauer polynomials is given by

$$G_\lambda^n(y) = \left(\frac{-1}{2}\right)^n \frac{\Gamma(\lambda+\frac{1}{2})\Gamma(n+2\lambda)}{n!\Gamma(2\lambda)\Gamma\left(n+\lambda+\frac{1}{2}\right)}(1-y^2)^{-\lambda+\frac{1}{2}}\frac{\mathrm{d}^n}{\mathrm{d}y^n}(1-y^2)^{n+\lambda-\frac{1}{2}}. \tag{7}$$

The Gegenbauer polynomials are orthogonal on the interval$[-1, 1]$ with respect to the weight function $w(x) = (1-y^2)^{\lambda-\frac{1}{2}}$.

$$\int_{-1}^{1}(1-y^2)^{\lambda-\frac{1}{2}}G_\lambda^m(y)G_\lambda^n(y)\mathrm{d}y = L_m^\lambda\delta_{mn}, \quad \lambda > \frac{-1}{2}, \tag{8}$$

where $L_m^\lambda = \frac{\pi 2^{1-2\lambda}\Gamma(m+2\lambda)}{m!(m+\lambda)(\Gamma\lambda)^2}$ is the normalizing factor and δ is the Kronecker delta function. This following inequality holds for Gegenbauer polynomials:

$$|G_\lambda^n(\cos\theta)|(\sin\theta)^\lambda < \frac{\Gamma(n+\frac{3\lambda}{2})2^{1-\lambda}}{\Gamma(\lambda)\Gamma(1+n+\frac{\lambda}{2})}, \quad 0 \le \theta \le \pi. \tag{9}$$

Another recurrence relation with integration is

$$\int G_\lambda^n(x)w(x)\mathrm{d}x = \frac{-2\lambda(1-x^2)^{\frac{1}{2}+\lambda}}{n(n+2\lambda)}G_{\lambda+1}^{n-1}(x). \tag{10}$$

We can define Gegenbauer wavelet on [0, 1]by

$$\psi_{n,m}^\lambda(x) = \begin{cases} \frac{1}{\sqrt{L_m^\lambda}}2^{\frac{k}{2}}G_\lambda^m(2^k x - \hat{n}), & \frac{\hat{n}-1}{2^k} < x < \frac{\hat{n}+1}{2^k} \\ 0 & \text{otherwise,} \end{cases} \tag{11}$$

where $k = 1, \ldots, n = 1, \ldots 2^{k-1}$, $\hat{n} = 2n-1$ is translation parameter, m in the order of Gegenbauer wavelet. For each λ a different family of wavelets can be generated. If we put $\lambda = 0$ and $\lambda = 1$, we get Chebyshev wavelets of the first and second kinds, respectively. Putting $\lambda = \frac{1}{2}$, we get the family of Legendre wavelets.

3 Function approximation

We can use Gegenbauer wavelet to expand any function $f(x)$ defined over [0, 1] as

$$f(x) = \sum_{n=0}^{\infty}\sum_{m=0}^{\infty} c_{nm}\psi_{n,m}^\lambda(x), \tag{12}$$

where $c_{pq} = \int_0^1 f(x)\psi_{n,m}^\lambda(x)w_n^\lambda(x)\mathrm{d}x$.

Here, $w_n^\lambda(x) = (1-(2^k x(2n-1))^2)^{\lambda-1/2}$ is the weight function. The truncated form of the above infinite series is

$$f(x) = \sum_{n=0}^{2^{k-1}}\sum_{m=0}^{M-1} c_{nm}\psi_{n,m}^\lambda(x) = C^T\Psi(x), \tag{13}$$

where C and $\Psi(x)$ are column vector of order $2^{k-1}M$. We can rewrite the above equation as

$$f(x) = \sum_{k=0}^{\hat{m}} c_k \psi_k^{\lambda}(x) = C^T \Psi(x), \tag{14}$$

where $\hat{m} = 2^{k-1}M$ and $k = Mn + m + 1$.

Similarly, an arbitrary function of two variables can be expanded in terms of Gegenbauer wavelet as

$$f(x,t) = \sum_{k=0}^{\hat{m}} \sum_{l=0}^{\hat{m}} c_{kl} \psi_k^{\lambda}(x) \psi_l^{\lambda}(t) = \Psi^T(x) V \Psi(t), \tag{15}$$

where $V = [c_{ij}]$ and $c_{ij} = \int_0^1 \int_0^1 f(x,t)\psi_i^{\lambda}(x)\psi_j^{\lambda}(t) w_n^{\lambda}(x) w_n^{\lambda}(t) \mathrm{d}x\mathrm{d}t$.

4 Error bound and stability analysis

In this section, we discuss the error analysis and derive an upper bound for the truncation error and also discuss convergence of the Gegenbauer wavelet.

Theorem 1 *A function $g(x) \in L^2[0,1]$ can be approximated as an infinite series of Gegenbauer wavelets. This series will converge uniformly to $g(x)$, with given condition $|g''(x)| \leq M$. Moreover, expansion coefficient given in Eq. (11) satisfies the inequality*

$$|c_{nm}| < \frac{4M(1+\lambda)^2(1+m+\lambda)^2}{n^{\frac{5}{2}}(m-2)^4}, \quad \forall n \geq 1, m > 2. \tag{16}$$

Proof With the help of the definition given in Eq. (10) and by the properties of the inner product, we can write coefficients c_{nm} as

$$c_{nm} = \frac{1}{\sqrt{L_m^{\lambda}}} 2^{\frac{k}{2}} \int_{\frac{n-1}{2^{k-1}}}^{\frac{n}{2^{k-1}}} g(x) G_{\lambda}^{m}(2^k x - 2n + 1) w(2^k x - n) \mathrm{d}x. \tag{17}$$

Integrating by parts of the right hand side of the above equation along with the property (9) of Gegenbauer wavelets, we get

$$\begin{aligned} c_{nm} = {} & \frac{\lambda 2^{\frac{6-k}{2}}}{m(m+2\lambda)\sqrt{L_m^{\lambda}}} \int_{\frac{n-1}{2^{k-1}}}^{\frac{n}{2^{k-1}}} g'(x) G_{\lambda-1}^{m-1}(2^k x - 2n + 1) \\ & (2^k x - n)(1 + n - 2^k t) w(2^k x - n) \mathrm{d}x. \end{aligned} \tag{18}$$

Again integrating by parts and substituting $2^k t - 2n + 1 = \cos\theta$, we can rewrite the above equation as

$$c_{nm} = \frac{2^{-2\lambda - \frac{5k-5}{2}} (\lambda)_2 \sqrt{2}}{(m-1)_2 (m-1+2\lambda)_2 \sqrt{L_m^{\lambda}}} \int_0^{\pi} g''\left(\frac{\cos\theta + 2n + 1}{2^k}\right) G_{\lambda-2}^{m-2}(\sin\theta)^{2\lambda+4} \cos\theta \mathrm{d}\theta. \tag{19}$$

Now, considering inequality (9) and assumption $|g''(x)| \leq M$, we get

$$|c_{nm}| \leq \frac{2^{-2\lambda - \frac{5k-5}{2}} |(\lambda)(\lambda+1)| \sqrt{2}}{(m-1)_2 (m-1+2\lambda)_2 |\sqrt{L_m^{\lambda}}|}$$

$$\times \int_0^{\pi} |g''(\frac{\cos\theta + 2n + 1}{2^k})||G_{\lambda-2}^{m-2}(\sin\theta)^{2\lambda+4}\cos\theta|\mathrm{d}\theta.$$

$$< \frac{M2^{-2\lambda-\frac{5k-5}{2}}|(\lambda)(\lambda+1)|\sqrt{2}}{(m-1)_2(m-1+2\lambda)_2|\sqrt{L_m^{\lambda}}|} \times \int_0^{\pi} |G_{\lambda-2}^{m-2}(\sin\theta)^{2\lambda+4}\cos\theta|\mathrm{d}\theta. \quad (20)$$

Putting the value of $\sqrt{L_m^{\lambda}}$, we have

$$|c_{nm}| < \frac{4M(\lambda+1+m)^2(1+\lambda)^2}{(m-2)^4 n^{\frac{5}{2}}},$$

which completes the proof of the theorem. □

Next for the error bound, let us consider a function $u(x,t) \in C^M[0,1]$ where $(x,t) \in [0,1]\times[0,1]$. Consider

$$\Theta_M = \mathrm{Span}\{G_i^{\lambda}G_j^{\lambda}, \quad i,j = 0,1\ldots M-1\}. \quad (21)$$

Assuming $\|u(x,t) \in \Theta_M$ is a better approximation of $u(x,t)$, we obtain

$$\|u(x,t) - \tilde{u}(x,t)\| \le \|u(x,t) - w(x,t)\|, \forall w(x,t) \in \Theta_M. \quad (22)$$

Now following the procedure as given in De Villiers (2012), Gasca and Sauer (2001), we have

$$u(x,t) - w(x,t) = \frac{1}{M!}\frac{\partial^M u(\varsigma,t)}{\partial x^M}\prod_{i=1}^{M-1}(x-x_i) + \frac{1}{M!}\frac{\partial^M u(x,\tau)}{\partial t^M}\prod_{i=1}^{M-1}(t-t_j)$$
$$- \frac{1}{(M!)^2}\frac{\partial^{2M}u(\varsigma',\tau')}{\partial x^M\partial t^M}\prod_{j=1}^{M-1}(t-t_j)\prod_{i=1}^{M-1}(x-x_i),$$

where ς, τ, ς',$\tau' \in [0,1]$, x_i and t_j are roots of G_M^{λ}.

Now,

$$\|u(x,t) - w(x,t)\| \le \frac{1}{M!}\max_{(x,t)}\left|\frac{\partial^M u}{\partial x^M}\right|\left\|\prod_{i=1}^{M-1}(x-x_i)\right\| + \frac{1}{M!}\max_{(x,t)}\left|\frac{\partial^M u}{\partial t^M}\right|\left\|\prod_{i=1}^{M-1}(t-t_j)\right\|$$
$$- \frac{1}{(M!)^2}\max_{(x,t)}\left|\frac{\partial^{2M}u}{\partial x^M\partial t^M}\right|\left\|\prod_{j=1}^{M-1}(t-t_j)\right\|\left\|\prod_{i=1}^{M-1}(x-x_i)\right\|. \quad (23)$$

As $u(x,t) \in C^M[0,1]$, we can say that there exist N_1, N_2 and N_3 such that

$$\max_{(x,t)}\left|\frac{\partial^M u}{\partial x^M}\right| \le N_1, \max_{(x,t)}\left|\frac{\partial^M u}{\partial t^M}\right| \le N_2, \max_{(x,t)}\left|\frac{\partial^{2M}u}{\partial x^M\partial t^M}\right| \le N_3. \quad (24)$$

By minimizing the factor $\|\prod_{i=1}^{M-1}(x-x_i)\|$, we have

$$\|u(x,t) - \tilde{u}(x,t)\| \le N_3\frac{4}{(M!)^2 4^{2M}} + (N_1+N_2)\frac{4}{(M!)4^M} = H(N_1,N_2,N_3,M). \quad (25)$$

Thus, we have derived an upper bound of the Gegenbauer polynomial for the absolute error.

Theorem 2 *Let $u(x,t) \in C^M[0,1]$ be defined on domain $(x,t) \in [0,1] \times [0,1]$ with*

$$\max_{(x,t)} \left| \frac{\partial^M u}{\partial x^M} \right| \leq N_1, \max_{(x,t)} \left| \frac{\partial^M u}{\partial t^M} \right| \leq N_2, \max_{(x,t)} \left| \frac{\partial^{2M} u}{\partial x^M \partial t^M} \right| \leq N_3, \tag{26}$$

where N_1, N_2 and N_3 are constants. If $u(x,t)$ has Gegenbauer wavelet expansion as $\Psi^T(x) V \Psi(t)$ then error bound is given by

$$\|u(x,t) - \Psi^T(x) V \Psi(t)\| \leq H(N_1, N_2, N_3, M) \frac{\sqrt{\pi}}{2^{\frac{k+1}{2}}} \frac{\Gamma(\frac{1}{2}+\lambda)}{\Gamma(1+\lambda)}. \tag{27}$$

Proof By the orthogonality condition of Gegenbauer wavelet, we have

$$\|u(x,t) - \Psi^T(x) V \Psi(t)\|^2 = \int_0^1 \int_0^1 w_n^\lambda(x) w_n^\lambda(t) (u(x,t) - \Psi^T(x) V \Psi(t))^2 \mathrm{d}x \mathrm{d}t.$$

Since we have divided the domain into 2^{2k} subdomains, we get

$$\begin{aligned} \|u(x,t) - \Psi^T(x) V \Psi(t)\|^2 &= \sum_{n=0}^{2^{k-1}} \sum_{n'=0}^{2^{k-1}} \int_{\frac{n-1}{2^{k-1}}}^{\frac{n}{2^{k-1}}} \int_{\frac{n'-1}{2^{k-1}}}^{\frac{n'}{2^{k-1}}} w_n^\lambda(x) w_n^\lambda(t) (u(x,t) \\ &\quad - \Psi^T(x) V \Psi(t))^2 \mathrm{d}x \mathrm{d}t \\ &\leq \sum_{n=0}^{2^{k-1}} \sum_{n'=0}^{2^{k-1}} \int_{\frac{n-1}{2^{k-1}}}^{\frac{n}{2^{k-1}}} \int_{\frac{n'-1}{2^{k-1}}}^{\frac{n'}{2^{k-1}}} w_n^\lambda(x) w_n^\lambda(t) (u(x,t) \\ &\quad - \tilde{u}(x,t)^2 \mathrm{d}x \mathrm{d}t, \end{aligned}$$

where $\tilde{u}(x,t)$ satisfies the error bound given in Eq. (26). So we have

$$\begin{aligned} &\|u(x,t) - \Psi^T(x) V \Psi(t)\|^2 \\ &\leq (H(N_1, N_2, N_3, M))^2 \sum_{n=0}^{2^{k-1}} \sum_{n'=0}^{2^{k-1}} \int_{\frac{n-1}{2^{k-1}}}^{\frac{n}{2^{k-1}}} \int_{\frac{n'-1}{2^{k-1}}}^{\frac{n'}{2^{k-1}}} w_n^\lambda(x) w_n^\lambda(t) \mathrm{d}x \mathrm{d}t \\ &\leq (H(N_1, N_2, N_3, M))^2 \frac{\pi}{2^{k+1}} \frac{\Gamma(\frac{1}{2}+\lambda)^2}{\Gamma(1+\lambda)^2}, \end{aligned}$$

which completes the proof of the theorem. □

5 Operational matrix of the derivative

Theorem 3 *If $\Psi(t)$ denotes the Gegenbauer wavelet, then the derivative of $\Psi(t)$ can be written as*

$$\frac{\mathrm{d}}{\mathrm{d}x} \Psi(t) = D \Psi(t), \tag{28}$$

where D is an operational matrix of order $2^{k-1}M$ which can be defined as

$$D = \begin{bmatrix} \theta & 0 & 0 & \cdots & 0 \\ 0 & \theta & 0 & \cdots & 0 \\ 0 & 0 & \theta & \cdots & 0 \\ \vdots & \vdots & \cdots & \vdots & \\ 0 & 0 & 0 & \cdots & \theta \end{bmatrix},$$

where θ is a matrix of order $M \times M$ having (l, m)th elements defined as

$$\theta_{h,k} = \begin{cases} \frac{2^{m+1}(m+\lambda-1)}{\sqrt{\frac{(m-1+\lambda)\Gamma(m)\Gamma(h-1+2\lambda)}{(l-1+\lambda)\Gamma(l)\Gamma(m-1+2\lambda)}}}, & l = 2, \ldots, M, \quad k = 1, \ldots, l-1 \quad \text{and} \quad (l+m)\text{odd} \\ 0, & \text{otherwise}. \end{cases} \tag{29}$$

In general, n-times derivative of vector $\Psi(x)$ is expressed by

$$\frac{\mathrm{d}^n}{\mathrm{d}x^n}\Psi(x) = D^n\Psi(x), \tag{30}$$

where D^n is the n-th power of D.

5.1 Gegenbauer wavelet operational matrix of variable-order fractional derivative

Type 1 fractional derivative of variable-order $(q-1) < \gamma(x,t) \leq q$ of a Gegenbauer vector $\Psi(t)$ can be defined as

$${}_0D_t^{\gamma(x,t)}\Psi(t) \simeq Q_t^{\gamma(x,t)}\Psi(t), \tag{31}$$

where $Q_t^{\gamma(x,t)}$ is an $\hat{m} \times \hat{m}$ operational matrix of variable order for Gegenbauer wavelet. To derive explicit form of this matrix we introduce another family of piecewise functions, which are defined on [0, 1] as

$$\omega_{nm}(t) = \begin{cases} t^m, & t \in [\frac{n}{2^k}, \frac{n+1}{2^k}], \\ 0, & \text{otherwise}, \end{cases} \tag{32}$$

for $n = 0, 1, \ldots, 2^{k-1}$, $m = 0, 1, \ldots, M-1$. An $\hat{m}$ set of these non-normalized functions can be expressed as

$$\Omega(t) = [\omega_1(t), \omega_2(t), \ldots, \omega_{\hat{m}}(t)]^T, \tag{33}$$

where $\omega_i(t) = \omega_{nm}(t)$ and index i can be determined by $i = Mn + m + 1$. If $\Omega(t)$ and $\Psi(t)$ are vectors defined in Eqs. (13) and (32), then

$$\Omega(t) = P\Psi(t), \tag{34}$$

where $P = [p_{ij}]$ is $\hat{m} \times \hat{m}$ order matrix whose elements are determined by $p_{ij} = \langle \omega_i(t), \psi_j(t) \rangle$.

Lemma *Let $\Omega(t)$ be the vector defined in Eq. (25) and $(q-1) < \gamma(x,t) \leq q$ be a positive function defined on [0, 1]. Then V1 type fractional derivative of variable-order $\gamma(x,t)$ of $\omega_{nm}(t)$ can be expressed as*

$${}_0D_t^{\gamma(x,t)}\omega_{nm}(t) = \begin{cases} \frac{m!}{\Gamma(m-\gamma(x,t)+1)}t^{m-\gamma(x,t)}, & m = q, q+1, \ldots, M-1, \quad t \in [\frac{n}{2^k}, \frac{n+1}{2^k}], \\ 0, & \text{otherwise}. \end{cases} \tag{35}$$

Proof Using relation (4) it can be proved easily. □

Theorem 4 *Let us assume $\Omega(t)$ to be the vector which is defined in Eq. (25) and $(q-1) < \gamma(x,t) \leq q$ a positive function defined over [0, 1]. Then fractional derivative of variable order of type 1 of $\Omega(t)$ can be defined as*

$${}_0D_t^{\gamma(x,t)}\Omega(t) = V_t^{\gamma(x,t)}\Omega(t), \tag{36}$$

where $V_t^{\gamma(x,t)}$ *is a matrix of order* $\hat{m} \times \hat{m}$ *which can be defined by*

$$V_t^{\gamma(x,t)} = \begin{bmatrix} S_t^{\gamma(x,t)} & 0 & 0 & \cdots & 0 \\ 0 & S_t^{\gamma(x,t)} & 0 & \cdots & 0 \\ 0 & 0 & S_t^{\gamma(x,t)} & \cdots & 0 \\ \vdots & \vdots & \cdots & \vdots & \\ 0 & 0 & 0 & \cdots & S_t^{\gamma(x,t)} \end{bmatrix},$$

where $S_t^{\gamma(x,t)}$ *is an* $M \times M$ *matrix given by*

$$S_t^{\gamma(x,t)} = t^{-\gamma(x,t)} \begin{bmatrix} 0 & 0 & \cdots & 0 & & & & \\ \vdots & \vdots & \cdots & \vdots & & & & \\ 0 & 0 & \cdots & 0 & & & & \\ 0 & \cdots & 0 & \frac{q!}{\Gamma(q-\gamma(x,t)+1)} & 0 & 0 & \cdots & 0 \\ 0 & \cdots & 0 & 0 & \frac{(q+1)!}{\Gamma(q-\gamma(x,t)+2)} & 0 & \cdots & 0 \\ \vdots & \vdots & \cdots & \vdots & & & & \\ \vdots & \vdots & \vdots & \vdots & \vdots & \vdots & \frac{(M-1)!}{\Gamma(M-\gamma(x,t)+2)} & 0 \\ 0 & 0 & 0 & 0 & \cdots & 0 & 0 & \frac{M!}{\Gamma(M-\gamma(x,t)+1)} \end{bmatrix}.$$

Proof By using the above lemma, the proof becomes very straightforward. □

Theorem 5 *Let* $\Psi(t)$ *be the Gegenbauer vector defined in Eq.* (10) *and* $(q-1) < \gamma(x,t) \leq q$ *be a positive function defined on* $[0,1]$. *Then the variable-order fractional derivative of* $\Psi(t)$ *is given as*

$${}_0D_t^{\gamma(x,t)}\Psi(t) = Q_t^{\gamma(x,t)}\Psi(t) = (P^{-1}V_t^{\gamma(x,t)}P)\Psi(t). \tag{37}$$

Proof By considering Eq. (33) and Theorem 4,

$$\Psi(t) = P^{-1}\Omega(t), \tag{38}$$

and thus

$${}_0D_t^{\gamma(x,t)}\Psi(t) = P^{-1}{}_0D_t^{\gamma(x,t)}\Omega(t) = P^{-1}V_t^{\gamma(x,t)}\Omega(t) = (P^{-1}V_t^{\gamma(x,t)}P)\Psi(t), \tag{39}$$

which shows the proof of theorem. □

6 Proposed model

In the past decades, constant-order fractional model of diffusion equation has been considered and achieved success in many fields. For more complicated and realistic stochastic diffusion process (Chechkin et al. 2005), it became clear that more theoretical and numerical studies are needed. Many problems of physical, biological and physiological diffusion phenomena are not equipped to be characterized by the CO fractional diffusion equation. These phenomena are complex and analysis and diffusion behaviors are changed with time evolution, space variation or on system parameters. Such kind of phenomena exist in various fields such as plasma physics, biophysics, protein dynamics (Anh et al. 2005) and econophysics (Chechkin et al. 2008). In several diffusion processes, the diffusion rate decreases with the increase in time from normal diffusion to subdiffusion. So, to characterize for this type of diffusion

phenomena, a time-dependent variable-order model is a good choice. Diffusion in complex medium is a fast developing issue of research. Constant-order diffusion model can describe the diffusion phenomena in homogeneous medium. But in complex medium, the heterogeneities of the medium cause variations of permeability in different spatial positions. For this type of situation, variable-order model with space dependence is best approached, by which we can explain the location-dependent diffusion process. In addition, when studying diffusion process in a porous media when external field or medium structure varies with time, then the constant-order model cannot be used to characterize this phenomenon. When the groundwater problem is considered in a medium through which heterogeneous flow occurs and changes with time, VO reaction diffusion model is suggested. In this article as a first model we take space time variable-order reaction diffusion equation given by the following equation

$$ {}_0D_t^{\gamma(x,t)}u(x,t) = {}_0D_x^{\mu(x,t)}u(x,t) + \kappa(u(x,t)) + f(x,t), \tag{40} $$

with initial and boundary conditions as

$$ u(x,0) = f_1(x), u(0,t) = g_1(t), u(1,t) = g_2(t), \tag{41} $$

where $\kappa(u(x,t))$ is a source term. We take Galilei invariant advection–diffusion with a nonlinear source term as a second model given by

$$ \frac{\partial u(x,t)}{\partial t} + \frac{\partial u(x,t)}{\partial x} = D_t^{1-\gamma(x,t)}\left(\frac{\partial^2 u}{\partial x^2}\right) + R(x,t,u), \tag{42} $$

with initial and boundary condition as

$$ u(x,0) = f_2(x), u(0,t) = g_3(t), u(1,t) = g_4(t). \tag{43} $$

This variable-order advection–diffusion model can present a more effective mathematical framework for description of different real-world anomalous diffusion process.

7 Description of the proposed method

In this section, Gegenbauer wavelet and their operational matrices are used to solve model (40) and (42). First, we approximate the unknown function $u(x,t)$ by Gegenbauer wavelet as

$$ u(x,t) = \Psi(x)^T.U.\Psi(t). \tag{44} $$

Differentiating Eq. (36) with respect to x and t, we get

$$ \frac{\partial}{\partial x}u(x,t) = (D.\Psi(x))^T.U.\Psi(t), \tag{45} $$

$$ \frac{\partial}{\partial t}u(x,t) = \Psi(x)^T.U.D.\Psi(t), \tag{46} $$

$$ \frac{\partial^2}{\partial x^2}u(x,t) = \Psi(x)^T.U.D^2.\Psi(t). \tag{47} $$

Applying variable-order fractional derivative of order $\gamma(x,t)$ with respect to t in Eq. (44), we obtain

$$ {}_0D_t^{\gamma(x,t)}u(x,t) = \Psi(x)^T.U.Q_t^{\gamma(x,t)}.\Psi(t), \tag{48} $$

and also applying with respect to x,

$$ {}_0D_x^{\gamma(x,t)}u(x,t) = (Q_x^{\gamma(x,t)}.\Psi(x))^T.U.\Psi(t). \tag{49} $$

Putting the values of $u(x,t)$, $\frac{\partial}{\partial x}u(x,t)$, $\frac{\partial}{\partial t}u(x,t)$, $\frac{\partial^2}{\partial x^2}u(x,t)$, ${}_0D_t^{\gamma(x,t)}u(x,t)$ from Eqs. (44)–(47) in the given first model (40), we get

$$ \xi_1(x,t) = \Psi(x)^T.U.V_t^{\gamma(x,t)}.\Psi(t) - (D^2\Psi(x))^T.U.\Psi(t) - f(x,t), \tag{50} $$

and substituting those in the second model we get

$$ \begin{aligned} \xi_2(x,t) = {} & (\Psi(x))^T.U.D.\Psi(t) + (D.\Psi(x))^T.U.\Psi(t) - (D^2\Psi(x))^T.U.V_t^{1-\gamma(x,t)}.\Psi(t) \\ & - R(x,t,\Psi(x)^T.U.\Psi(t)). \end{aligned} \tag{51} $$

Using Eq. (44) in the prescribed initial and boundary conditions given in Eq. (41), we get

$$ \begin{aligned} \Psi(x)^T.U.\Psi(0) - f_1(x) &= 0, \\ \Psi(0)^T.U.\Psi(t) - g_1(t) &= 0, \\ \Psi(1)^T.U.\Psi(t) - g_2(t) &= 0, \end{aligned} \tag{52} $$

and from initial and boundary conditions given in Eq. (42), we get

$$ \begin{aligned} \Psi(x)^T.U.\Psi(0) - f_2(x) &= 0, \\ \Psi(0)^T.U.\Psi(t) - g_3(t) &= 0, \\ \Psi(1)^T.U.\Psi(t) - g_4(t) &= 0. \end{aligned} \tag{53} $$

To obtain an approximate solution, we have to find out the unknown matrix U. We collocate Eqs. (50) and (52) at points $x, t = 0, \frac{1}{\hat{m}}, \frac{2}{\hat{m}} \ldots, \frac{\hat{m}-1}{\hat{m}}$, and solve this non-linear system of equations to find U. After finding U, we can easily get the numerical solutions of both the models up to the desired degrees of accuracy.

8 Results and discussion

In this section, the validity of the method is shown through applying it on various examples of both the types of models having exact solutions with prescribed initial and boundary conditions. All numerical computations are done using Wolfram Mathematica version-11.3.

Example 1 We consider $\gamma(x,t) = \frac{2+sin(xt)}{4}$, $f(x,t) = 20x^2(1-x)\Big(\frac{t^{2-\gamma(x,t)}}{\Gamma(3-\gamma(x,t))} + \frac{t^{1-\gamma(x,t)}}{\Gamma(2-\gamma(x,t))}\Big)$, $\kappa(u) = 0$ and $\mu(x,t) = 2$ so that our model (40) is reduced to

$$ {}_0D_t^{\gamma(x,t)}u(x,t) = \frac{\partial^2 u(x,t)}{\partial x^2} + f(x,t). \tag{54} $$

Equation (54) with the aid of initial and boundary conditions

$$ u(x,0) = 10x^2(1-x), u(0,t) = 0, u(1,t) = 0 \tag{55} $$

gives the exact solution as $u(x,t) = 10x^2(1-x)(t+1)^2$ (Shen et al. 2012).

The graphs of numerical and exact solutions for $\hat{m} = 4$ are shown in Fig. 1. The absolute error for various $\hat{m}$ is shown in Table 1. The results clearly predict that our numerical results are in complete agreement with the existing results. From Table 2, it is found that the error obtained

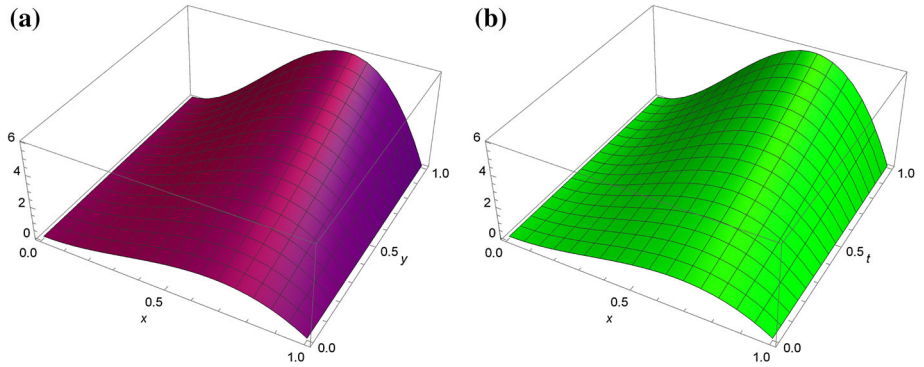

Fig. 1 Plots of $u(x,t)$ for $\hat{m}=4$ and $\lambda=2$ in case of numerical and exact solution for $t=0.5$

Table 1 Variations of absolute error for different x at $t=0.5$,$\lambda=2$ and various $\hat{m}$

$x\downarrow$	$\hat{m}=4$	$\hat{m}=6$	$\hat{m}=8$
0.2	3.2×10^{-14}	4.4×10^{-15}	1.88×10^{-15}
0.4	2.1×10^{-14}	1.7×10^{-15}	2.2×10^{-15}
0.6	1.2×10^{-14}	1.8×10^{-15}	3.1×10^{-15}
0.8	6.7×10^{-15}	2.2×10^{-15}	2.67×10^{-15}

Table 2 Comparison of absolute error for the method given in Shen et al. (2012) and our method for different x at $t=1$

$x\downarrow$	Method in Shen et al. (2012)	Our method
0.2	5.9×10^{-5}	4.4×10^{-16}
0.3	8.8×10^{-5}	1.3×10^{-15}
0.4	1.1×10^{-4}	8.8×10^{-16}
0.6	1.3×10^{-4}	1.7×10^{-15}
0.7	1.2×10^{-4}	1.8×10^{-15}
0.8	1×10^{-4}	8.8×10^{-16}
0.9	5.6×10^{-5}	7.5×10^{-15}

by our proposed method is more accurate compared to the existing numerical method (Shen et al. 2012).

Example 2 If we consider $\gamma(x,t)=1$, $\mu(x,t)=\frac{6+xt}{4}$ so that our model (40) is reduced to

$$\frac{\partial u}{\partial t}-{}_0D_x^{\mu(x,t)}u(x,t)+x\sin u=f(x,t), \tag{56}$$

which under the prescribed initial and boundary conditions

$$u(x,0)=6,\ u(0,t)=6,\ u(1,t)=6+t, \tag{57}$$

gives the exact solution as $u(x,t)=(x^{3.2}-2x^{4.2}+x^{5.2})(t+t^2)+xt+6$ (Li and Wu 2018) by choosing the proper value of $f(x,t)$.

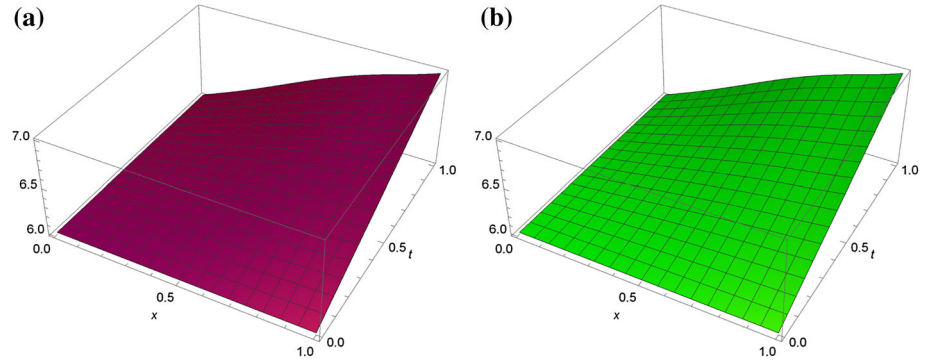

Fig. 2 Plots of $u(x,t)$ for $\hat{m}=4$ and $\lambda=2$ in case of numerical and exact solution for $t=0.5$

Table 3 Variations of absolute error for different x at $t=0.5$, $\lambda=2$ and various $\hat{m}$

$x\downarrow$	$\hat{m}=4$	$\hat{m}=6$	$\hat{m}=8$
0.2	3.4×10^{-13}	2.6×10^{-14}	4.8×10^{-15}
0.4	9.7×10^{-13}	5.4×10^{-14}	4.0×10^{-15}
0.6	1.5×10^{-12}	7.7×10^{-14}	1.4×10^{-15}
0.8	2.1×10^{-12}	9.2×10^{-14}	2.4×10^{-15}

Table 4 Comparison of absolute error for method given in Li and Wu (2018) and our method

$(x,t)\downarrow$	Method given in Li and Wu (2018)	Our method
(0.1, 0.1)	2.65×10^{-6}	2.1×10^{-15}
(0.3, 0.3)	5.67×10^{-5}	2.4×10^{-15}
(0.5, 0.5)	6.22×10^{-5}	2.9×10^{-15}
(0.7, 0.7)	3.75×10^{-4}	7.4×10^{-15}
(0.9, 0.9)	4.16×10^{-4}	9.9×10^{-15}

The absolute error for various $\hat{m}$ is shown in Table 2. The graphs of numerical and exact solutions for $\hat{m}=4$ are shown in Fig. 2 which clearly predict that our numerical results are in complete agreement with the existing results (Tables 3, 4).

Example 3 If we take $\gamma(x,t)=\frac{2+\sin(t)}{400}$, $f(x,t)=\frac{\Gamma(\beta+1)}{\Gamma(\beta+1-\gamma(x,t))}$, $\kappa(u)=\frac{u}{4}$ and $\mu(x,t)=2$, then our model (40) is reduced to

$$ {}_0D_t^{\gamma(x,t)}u(x,t)=\frac{\partial^2u(x,t)}{\partial x^2}+\frac{u}{4}+f(x,t). \tag{58}$$

Equation (58) with initial and boundary conditions

$$ u(x,0)=0,\ u(0,t)=0,\ u(1,t)=t^{\beta}, \tag{59}$$

gives the exact solution $u(x,t)=t^{\beta}\sin(\frac{x}{2})$ (Hajipour et al. 2019).

The graphs of numerical and exact solutions for $\hat{m}=4$ are shown in Fig. 3 and the absolute error is shown in Table 5. The results clearly predict that our numerical results are in complete agreement with the existing results. It is seen from the Table 6 that our proposed method is

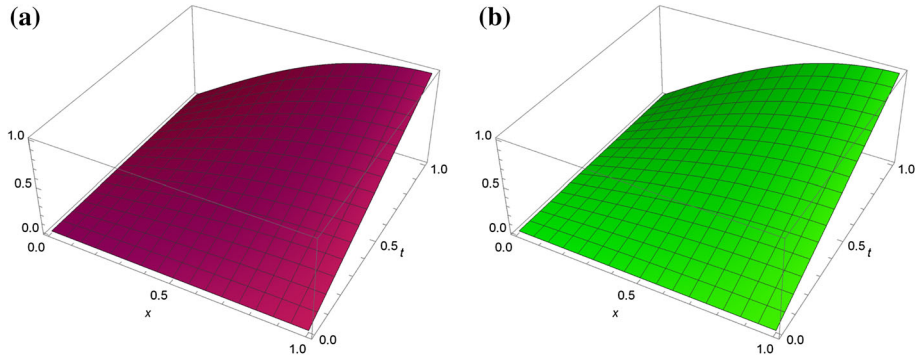

Fig. 3 Plots of $u(x,t)$ for $\hat{m}=4$ and $\lambda=2$ in case of numerical and exact solution for $t=0.5$

Table 5 Variations of absolute errors for different x at $t=0.5$, $\lambda=2$ and various $\hat{m}$

$x\downarrow$	$\hat{m}=4$	$\hat{m}=6$	$\hat{m}=8$
0.2	1.9×10^{-3}	2.8×10^{-5}	1.8×10^{-7}
0.4	1.6×10^{-3}	2.1×10^{-5}	1.5×10^{-7}
0.6	1.9×10^{-3}	2.3×10^{-5}	1.6×10^{-7}
0.8	2.6×10^{-3}	3.3×10^{-5}	2.2×10^{-7}

Table 6 Comparison of L_∞ errors for the method given in Hajipour et al. (2019) and our method

$M\downarrow$	Method in Hajipour et al. (2019)	Our method
4	3.86×10^{-2}	2.8×10^{-3}
8	4.23×10^{-3}	3.1×10^{-7}

much superior as compared to the existing numerical method (Hajipour et al. 2019) when maximum absolute error is computed for the given example.

Example 4 Taking $\gamma(x,t)=2x$, $\kappa(u)=cu(1-\frac{u^3}{3})$ and $\mu(x,t)=2t$ so that we get the following variable-order space and time, both fractional example

$$ {}_0D_t^{2x}u(x,t) = {}_0D_x^{2t}u(x,t)+cu\left(1-\frac{u^3}{3}\right)+f(x,t), \tag{60}$$

with initial and boundary condition as

$$u(x,0)=0, u(0,t)=0, u(1,t)=t, \tag{61}$$

and $f(x,t)$ is chosen such that the exact solution of the above the problem is $u(x,t)=xt$. The graphs of numerical and exact solutions for $\hat{m}=4$ are shown in Fig. 4. The results of absolute error given in Table 7 clearly predict that the error between the numerical solution and the exact solution decreases as the degree of approximation increases.

The VORDE characterizes the behavior of reaction and diffusion of pollutants in groundwater. Here, we assume that the concentration of pollutants is zero at time $t=0$. At the initial boundary $x=0$, the concentration of the pollutant is zero and increases linearly toward the boundary $x=1$. From Fig. 5, the case $c=0$ represents when the pollutant has no reaction

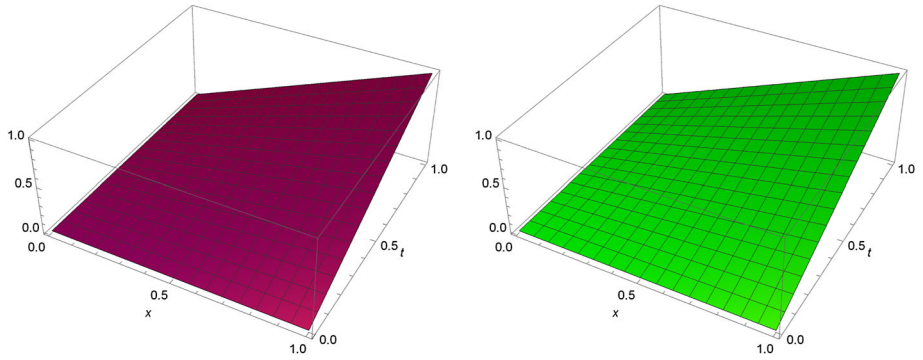

Fig. 4 Plots of $u(x,t)$ for $\hat{m}=4$ and $\lambda=2$ in case of numerical and exact solution for $t=0.5$

Table 7 Variations of absolute error for different x at $t=0.5$, $\lambda=2$ and various $\hat{m}$

$x\downarrow$	$\hat{m}=4$	$\hat{m}=6$	$\hat{m}=8$
0.2	1.7×10^{-6}	1.2×10^{-10}	1.3×10^{-12}
0.4	5.8×10^{-6}	4.9×10^{-10}	4.9×10^{-12}
0.6	1×10^{-5}	9.7×10^{-9}	9.5×10^{-11}
0.8	1.4×10^{-5}	1.4×10^{-9}	1.8×10^{-11}

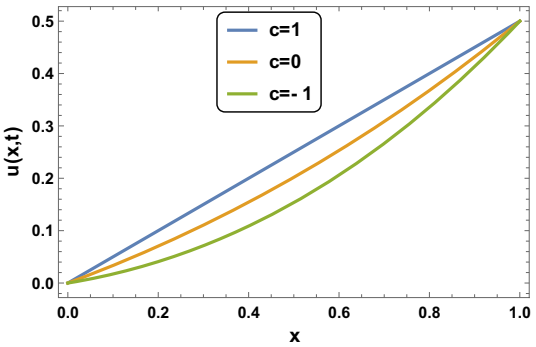

Fig. 5 Behavior of $u(x,t)$ for $\hat{m}=4$ and $\lambda=2$ at $t=0.5$

with groundwater, while $c=1$ (source term) and $c=-1$ (sink term) represent the cases when it reacts with groundwater. It is observed that in case of $c=1$, the concentration of the pollutant is more than when the pollutant has no reaction with groundwater, while in case of $c=-1$ the behavior of the solution is opposite. Figure 5 also shows that the concentration decreases at invasive fronts of the site. Figure 6 depicts that at time $t=0$, the concentration is zero and its growth increases with time.

Figure 7 depicts the fact that the pollutant concentration decreases when we add an accession to the variable-order exponent of time($\gamma(x,t)$), while the concentration is more if we give a shrinkage of amount 0.4 to $\gamma(x,t)$). It also shows that this growth and reduction of concentration are higher around the middle of the site as compared to the invasive fronts.

Example 5 If we take $\gamma(x,t)=\frac{10-tx}{300}$, $R(x,t,u)=u-u^2+e^x t\left(2+e^x t^3-2\frac{t^{\gamma(x,t)}}{\Gamma(2+\gamma(x,t))}\right)$, our model (42) is reduced to

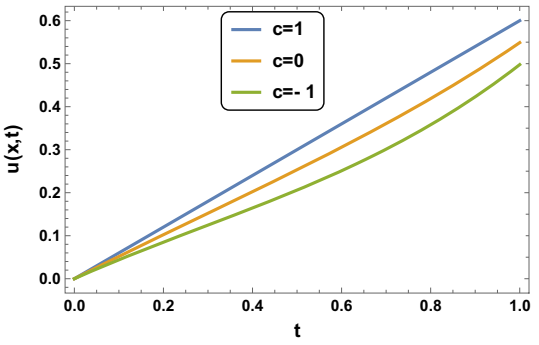

Fig. 6 Behaviour of $u(x,t)$ for $\hat{m}=4$ and $\lambda=2$ at $x=0.5$

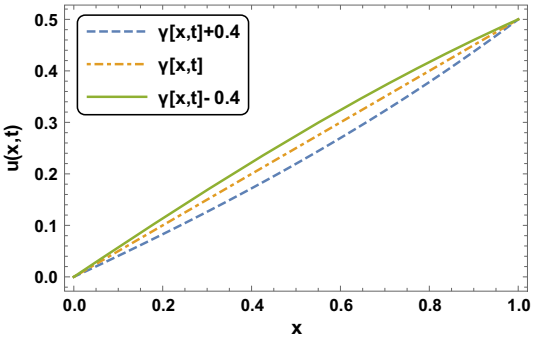

Fig. 7 Behaviour of $u(x,t)$ for $\hat{m}=4$ and $\lambda=2$ at $x=0.5$

$$\frac{\partial u(x,t)}{\partial t}+\frac{\partial u(x,t)}{\partial x}=D_t^{1-\gamma(x,t)}\left(\frac{\partial^2 u}{\partial x^2}\right)+R(x,t,u), \tag{62}$$

which with the aid of initial and boundary conditions as

$$u(x,0)=0, u(0,t)=t^2, u(1,t)=et^2, \tag{63}$$

gives the exact solution as $u(x,t)=t^2e^x$ (Abd-Elkawy and Alqahtani 2017).

The graphs of numerical and exact solutions for $\hat{m}=4$ are shown in Fig. 8. Here, the absolute error decreases steadily as the degree of approximation increases. The results clearly predict that our numerical results are in complete agreement with the existing results (Table 8).

Example 6 The model (34) with $\gamma(x,t)=\frac{1}{500}\left((tx)^2-sin^3tx+cos^4tx+266\right)$, $R(x,t,u)=u-u^2+te^{-2x}\left(t^3-2(t-1)e^x-\frac{2e^xt^{\gamma(x,t)}}{\Gamma(2+\gamma(x,t))}\right)$ is reduced to

$$\frac{\partial u(x,t)}{\partial t}+\frac{\partial u(x,t)}{\partial x}=D_t^{1-\gamma(x,t)}\left(\frac{\partial^2 u}{\partial x^2}\right)+R(x,t,u). \tag{64}$$

Equation (57) with initial and boundary conditions as

$$u(x,0)=0, u(0,t)=t^2, u(1,t)=e^{-1}t^2, \tag{65}$$

gives the exact solution as $u(x,t)=t^2e^{-x}$ (Abd-Elkawy and Alqahtani 2017).

The graphs of numerical and exact solutions for $\hat{m}=4$ are shown in Fig. 9. The results clearly predict that our numerical results are in complete agreement with the existing results. The absolute error between the exact and numerical solution is given in Table 9.

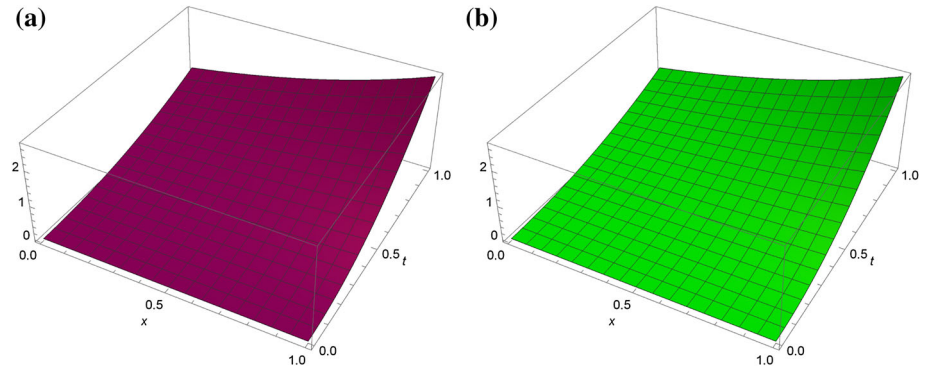

Fig. 8 Plots of $u(x,t)$ for $\hat{m}=4$ and $\lambda=2$ in case of numerical and exact solution for $t=0.5$

Table 8 Variations of absolute error for different x at $t=0.5$, $\lambda=2$ and various $\hat{m}$

$x\downarrow$	$\hat{m}=4$	$\hat{m}=6$	$\hat{m}=8$
0.2	5.7×10^{-4}	3.3×10^{-6}	9.1×10^{-9}
0.4	5.6×10^{-4}	3.2×10^{-6}	8.8×10^{-9}
0.6	5.8×10^{-4}	3.3×10^{-6}	9.1×10^{-9}
0.8	6.4×10^{-4}	3.6×10^{-6}	9.6×10^{-9}

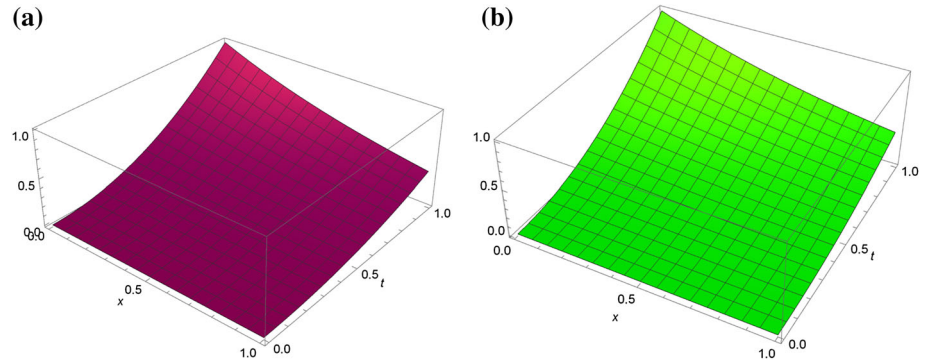

Fig. 9 The plots of $u(x,t)$ for $\hat{m}=4$ and $\lambda=2$ in case of numerical and exact solution for $t=0.5$

Table 9 Variations of absolute error for different x at $t=0.5$, $\lambda=2$ and various $\hat{m}$

$x\downarrow$	$\hat{m}=4$	$\hat{m}=6$	$\hat{m}=8$
0.2	2.3×10^{-4}	1.2×10^{-6}	3.4×10^{-9}
0.4	2.1×10^{-4}	1.1×10^{-6}	3.0×10^{-9}
0.6	1.9×10^{-4}	1×10^{-6}	2.9×10^{-9}
0.8	1.9×10^{-4}	1.1×10^{-6}	3×10^{-9}

9 Conclusion

In this article, we have achieved four important consequences. The first one is that the operational matrix for variable order is derived. The second one is the successful implementation of

the collocation method based on Gegenbauer wavelets to solve the variable-order non-linear reaction–diffusion equation and non-linear Galilei-invariant advection diffusion equation. The third one is finding the error bound and stability analysis of the proposed method. The last one is the graphical and tabular exhibitions to validate the effectiveness of the proposed method used for solving various linear/non-linear problems derived from two considered mathematical models for different particular cases. The beauty of the present contribution is the showing of the effect of the reaction term on the solute concentration for different particular cases.

Acknowledgements The authors are thankful to the revered reviewers for their valuable suggestions toward the improvement of the quality of the present article.

References

Abd-Elkawy MA, Alqahtani RT (2017) Space-time spectral collocation algorithm for the variable-order galilei invariant advection diffusion equations with a nonlinear source term. Math Model Anal 22(1):1–20

Anh VV, Angulo JM, Ruiz-Medina MD (2005) Diffusion on multifractals. Nonlinear Anal Theory Methods Appl 63(5–7):e2043–e2056

Chechkin AV, Gorenflo R, Sokolov IM (2005) Fractional diffusion in inhomogeneous media. J Phys A Math Gen 38(42):L679

Chechkin A, Gonchar VY, Gorenflo R, Korabel N, Sokolov I (2008) Generalized fractional diffusion equations for accelerating subdiffusion and truncated lévy flights. Phys Rev E 78(2):021111

Coimbra CF (2003) Mechanics with variable-order differential operators. Ann Phys 12(11–12):692–703

Couteron P, Lejeune O (2001) Periodic spotted patterns in semi-arid vegetation explained by a propagation-inhibition model. J Ecol 89(4):616–628

Dabiri A, Moghaddam BP, Machado JT (2018) Optimal variable-order fractional pid controllers for dynamical systems. J Comput Appl Math 339:40–48

Darania P, Ebadian A (2007) A method for the numerical solution of the integro-differential equations. Appl Math Comput 188:657–668

Das S, Singh A, Ong SH (2018) Numerical solution of fractional order advection-reaction-diffusion equation. Therm Sci 22:S309–S316

Das S, Vishal K, Gupta P (2011) Solution of the nonlinear fractional diffusion equation with absorbent term and external force. Appl Math Model 35(8):3970–3979

De Villiers J (2012) Mathematics of approximation, vol 1. Springer Science and Business Media, New York

Diethelm K, Ford NJ, Freed AD (2002) A predictor-corrector approach for the numerical solution of fractional differential equations. Nonlinear Dyn 29(1–4):3–22

Elgindy KT, Smith-Miles KA (2013) Solving boundary value problems, integral, and integro-differential equations using Gegenbauer integration matrices. J Comput Appl Math 237(1):307–325

Gasca M, Sauer T (2001) On the history of multivariate polynomial interpolation. In: Numerical analysis: historical developments in the 20th century. Elsevier, pp 135–147

Gürbüz B, Sezer M (2016) Laguerre polynomial solutions of a class of initial and boundary value problems arising in science and engineering fields. Acta Phys Pol A 130(1):194–197

Hajipour M, Jajarmi A, Baleanu D, Sun H (2019) On an accurate discretization of a variable-order fractional reaction-diffusion equation. Commun Nonlinear Sci Numer Simul 69:119–133

Hashim I, Abdulaziz O, Momani S (2009) Homotopy analysis method for fractional IVPS. Commun Nonlinear Sci Numer Simul 14(3):674–684

Jafari H, Yousefi S, Firoozjaee M, Momani S, Khalique CM (2011) Application of legendre wavelets for solving fractional differential equations. Comput Math Appl 62(3):1038–1045

Jaiswal S, Chopra M, Das S (2018) Numerical solution of two-dimensional solute transport system using operational matrices. Transp Porous Media 122(1):1–23

Keshi FK, Moghaddam BP, Aghili A (2018) A numerical approach for solving a class of variable-order fractional functional integral equations. Comput Appl Math 37(4):4821–4834

Kilbas A, Srivastava H, Trujillo JJ (2006) Theory and applications of the fractional differential equations, vol 204. Elsevier (North-Holland), Amsterdam

Kondo S (2009) How animals get their skin patterns: fish pigment pattern as a live turing wave. In: Systems biology. Springer, Berlin, pp 37–46

Kondo S, Asai R (1995) A reaction-diffusion wave on the skin of the marine angelfish pomacanthus. Nature 376(6543):765
Li Y, Sun N (2011) Numerical solution of fractional differential equations using the generalized block pulse operational matrix. Comput Math Appl 62(3):1046–1054
Li X, Wu B (2018) Iterative reproducing kernel method for nonlinear variable-order space fractional diffusion equations. Int J Comput Math 95(6–7):1210–1221
Li Y, Zhao W (2010) Haar wavelet operational matrix of fractional order integration and its applications in solving the fractional order differential equations. Appl Math Comput 216(8):2276–2285
Lin R, Liu F, Anh V, Turner I (2009) Stability and convergence of a new explicit finite-difference approximation for the variable-order nonlinear fractional diffusion equation. Appl Math Comput 212(2):435–445
Lv C, Xu C (2016) Error analysis of a high order method for time-fractional diffusion equations. SIAM J Sci Comput 38(5):A2699–A2724
Machado JT, Kiryakova V, Mainardi F (2011) Recent history of fractional calculus. Commun Nonlinear Sci Numer Simul 16(3):1140–1153
Machado JAT, Moghaddam BP (2018) A robust algorithm for nonlinear variable-order fractional control systems with delay. Int J Nonlinear Sci Numer Simul 19(3–4):231–238
Malesza W, Macias M, Sierociuk D (2019) Analytical solution of fractional variable order differential equations. J Comput Appl Math 348:214–236
Milici C, Draganescu G, Machado JT (2019) Introduction to fractional differential equations. Nonlinear systems and complexity. Springer, Switzerland. https://doi.org/10.1007/978-3-030-00895-6
Moghaddam BP, Machado JAT (2017a) A computational approach for the solution of a class of variable-order fractional integro-differential equations with weakly singular kernels. Fract Calculus Appl Anal 20(4):1023–1042
Moghaddam BP, Machado JAT (2017b) Extended algorithms for approximating variable order fractional derivatives with applications. J Sci Comput 71(3):1351–1374
Moghaddam BP, Machado JAT (2017c) Sm-algorithms for approximating the variable-order fractional derivative of high order. Fundam Inf 151(1–4):293–311
Moghaddam BP, Mostaghim ZS (2017) Modified finite difference method for solving fractional delay differential equations. Boletim da Sociedade Paranaense de Matemática 35(2):49–58
Moghaddam B, Machado J, Behforooz H (2017) An integro quadratic spline approach for a class of variable-order fractional initial value problems. Chaos Solitons Fractals 102:354–360
Moghaddam B, Dabiri A, Lopes AM, Machado JT (2019) Numerical solution of mixed-type fractional functional differential equations using modified lucas polynomials. Comput Appl Math 38(2):46
Murray JD (1981) A pre-pattern formation mechanism for animal coat markings. J Theor Biol 88(1):161–199
Odibat Z (2011) On legendre polynomial approximation with the vim or ham for numerical treatment of nonlinear fractional differential equations. J Comput Appl Math 235(9):2956–2968
Ortigueira MD, Valério D, Machado JT (2019) Variable order fractional systems. Commun Nonlinear Sci Numer Simul 71:231–243. https://doi.org/10.1016/j.cnsns.2018.12.003. http://www.sciencedirect.com/science/article/pii/S1007570418303782
Podlubny I (1998) Fractional differential equations, to methods of their solution and some of their applications. Fractional differential equations: an introduction to fractional derivatives. Academic Press, San Diego
Rehman MU, Saeed U (2015) Gegenbauer wavelets operational matrix method for fractional differential equations. J Korean Math Soc 52:1069–1096
Samko SG, Ross B (1993) Integration and differentiation to a variable fractional order. Integr Transforms Spec Funct 1(4):277–300
Shen S, Liu F, Chen J, Turner I, Anh V (2012) Numerical techniques for the variable order time fractional diffusion equation. Appl Math Comput 218(22):10861–10870
Soon CM, Coimbra CF, Kobayashi MH (2005) The variable viscoelasticity oscillator. Ann Phys 14(6):378–389
Suarez L, Shokooh A (1997) An eigenvector expansion method for the solution of motion containing fractional derivatives. ASME J Appl Mech 64:629–635
Sun H, Chen W, Wei H, Chen Y (2011) A comparative study of constant-order and variable-order fractional models in characterizing memory property of systems. Eur Phys J Spec Top 193(1):185
Tavares D, Almeida R, Torres DF (2016) Caputo derivatives of fractional variable order: numerical approximations. Commun Nonlinear Sci Numer Simul 35:69–87
Tripathi NK, Das S, Ong SH, Jafari H, Al Qurashi M (2016) Solution of higher order nonlinear time-fractional reaction diffusion equation. Entropy 18(9):329
Valério D, Sá da CJ (2013) Variable order fractional controllers. Asian J Control 15(3):648–657
Xiang M, Zhang B, Yang D (2019) Multiplicity results for variable-order fractional Laplacian equations with variable growth. Nonlinear Anal 178:190–204

Yuanlu L (2010) Solving a nonlinear fractional differential equation using Chebyshev wavelets. Commun Nonlinear Sci Numer Simul 15(9):2284–2292

Zayernouri M, Karniadakis GE (2015) Fractional spectral collocation methods for linear and nonlinear variable order FPDES. J Comput Phys 293:312–338